Patterning of ITO Layer on Glass with High Repetition Rate Picosecond Lasers

Gediminas RAČIUKAITIS, Marijus BRIKAS, Mindaugas GEDVILAS and Gediminas DARČIANOVAS

Laboratory for Applied Research, Institute of Physics, Savanoriu Ave. 231, LT-02300 Vilnius, Lithuania
E-mail: graciukaitis@ar.fi.lt

New high repetition rate picosecond lasers offer possibility for high efficiency structuring of transparent conductors on glass and other substrates. The results of ablation of the indium-tin oxide (ITO) layer on glass with picosecond lasers at various wavelengths are presented. Laser radiation initiated ablation that formed trenches in ITO. Profile of the trenches was analyzed with a phase contrast optical microscope, a stylus type profiler, SEM and AFM. Clean removal of the ITO layer with the 266 nm radiation was observed when laser fluence was above the threshold of 0.20 J/cm^2, while for the 355 nm radiation the threshold was higher, above 0.46 J/cm^2. The glass substrate was damaged in the area where the fluence was higher than 1.55 J/cm^2. The 532 nm radiation allowed getting well defined trenches, but a lot of residues in the form of dust were generated on the surface. Use of UV laser radiation with fluences close to the ablation threshold made it possible to minimize the recast ridge formation and surface contamination during the process. The latter was confirmed by the scanning Auger spectroscopy. The processing speed of up to 0.5 m/s was achieved when using high repetition rate picosecond lasers in the UV range.

Keywords: ITO on glass, laser ablation, picosecond laser, UV radiation

1. Introduction

Indium-tin oxide (ITO) is commonly used in flat panel displays and organics-based electronics as a transparent electrode. The conventional method of making patterns is photolithography which involves multiple processes: photoresist coating, exposure, developing, wet chemical etching, stripping and baking. Other alternative low-cost methods such as micro-contact printing are under investigation [1]. Laser direct write (LDW) is a competing technology that is intended to be used for patterning ITO. It is a maskless, dry process, replacing the numerous photolithographic process steps with one laser ablation operation. LDW is a flexible process that allows easy change of the contact pattern, making LDW the desired production method for the organic light emitting devices (OLED) application of the near future with the opportunity of customization: lighting systems for signage and dynamic advertisement [2]. Moreover, reel-to-reel production technologies of flexible electronics are looking for the reliable and easy to automate methods of contact patterning.

New types of devices boost strict specifications to the shape and accuracy of ITO processing. The well defined edges and good electrical isolation at a short separation between conductor lines are required for the modern OLED and radio frequency identification devices (RFID) [2]. Sharp edges of the ablated lines should be achieved for high resolution displays. This is especially important when the distance between the conductor lines shrinks down to 10 µm. Organic electronics devices are thin film structures with the total thickness of active layers in the range of 100 nm. Since organic layers in the device structure are extremely thin, ridges on edges could be the reason of shorts in the structure, causing reduction of the working longevity or efficiency of OLED devices.

Nano- and femtosecond lasers were applied to ITO ablation [3-7]. Patterning made with solid state nanosecond lasers provided good isolation required for photovoltaic applications [3]. High pulse energy enabled making the entire contact of display pixel by one laser pulse [4]. The material removal rate was high for nanosecond lasers, and the best results were obtained when the ITO layer and the glass substrate were absorbing at laser wavelength. [5]. The main drawback in using the laser direct write technologies for OLED are ridges on edges on the ablated trenches. They are formed by extruding the melted material by vapor pressure and also by spallation of the layer from the substrate [6]. Even the use of the F_2 excimer laser with extremely short wavelength of 157 nm and pulse duration of a few tens of nanoseconds led to formation of ridges on the trench edges [7]. Higher quality of processing can be achieved by ultra-fast laser pulses [8-10]. The processing speed is too slow with the up-to-date femtosecond lasers and the ridges still remained using IR radiation [8].

New high repetition rate short -pulse lasers offer possibility of high efficiency structuring of the transparent conductor on glass and other substrates. The results of ablation of the 120 nm thick ITO layer on glass with picosecond lasers at various wavelengths are presented. Pulse energy and overlap as well as focal position of the lens relative to the ITO surface were varied. Profile of the trenches formed by laser ablation was analyzed with a phase contrast optical microscope, a stylus type profiler, the scanning electron microscope (SEM) and the atomic force microscope (AFM).

Use of fluences close to the ablation threshold made it possible to minimize the recast ridge formation and surface

contamination during the process. The latter was confirmed by the scanning Auger spectroscopy. The processing speed of up to 0.5 m/s was achieved when using high repetition rate picosecond lasers in the UV range.

2. Experimental

Commercially available ITO glass (Optical Filter Ltd, UK) with resistance of 12-ohms/sq was used in the experiments. The soda lime float glass was coated with a primary smoothening layer of SiO_2, and the layer of indium-tin oxide was vacuum-deposited on it. The thickness of the ITO layer was 120 nm.

Two picosecond lasers with regenerative amplification were used in the ablation experiments: PL2241 with 60 ps pulse duration and 250 Hz pulse repetition rate, and PL10100 (10 ps, 100 kHz). Both lasers were made by Ekspla Ltd. Nonlinear crystals were used for wavelength conversion to UV. The objective with the focal length of 50 mm was used with the laser PL2241. The etching of narrow trenches in ITO was made by using the PL10100 laser and the objective with the focal length of 10 mm. Samples were moved by the XY stage with linear motors.

Various combinations of pulse energy, their overlap and wavelength were used for etching the contact separation lines in ITO. Series of samples were prepared by ablating trenches in ITO with picosecond lasers, varying the wavelength of radiation (1064 nm, 532 nm, 355 nm and 266 nm). Point-by-point technique with different settings of motion between shots (step) was used to form isolating lines in the film. The parameters used in experiments are presented in Tables 1 and 2. In addition, the fluence of laser radiation was varied by control of the focal position of an objective. The range of the up-down movement was limited to ± 2.0 mm (50 mm) and ± 0.4 mm (10 mm) for different objectives. The fluence decreased with the increase in the beam diameter. However, a larger diameter at a constant positioning speed led to a higher pulse overlap. Shift of the 50-mm objective by the distance of 2 mm changed the spot overlap five times.

Table 1 Samples of ITO on the glass substrate prepared with the PL2241 laser: laser wavelength, pulse energy and step between pulses by processing a line.

λ, nm	step, μm / energy, μJ	1	2	5	10
266	8	#1	#2	#3	#4
	20	#5	#6	#7	#8
	40	#9	#10	#11	#12
	80	#13	#14	#15	#16
355	8	#17	#18	#19	#20
	20	#21	#22	#23	#24
	40	#25	#26	#27	#28
	80	#29	#30	#31	#32
532	40	#33	#34	#35	#36
	80	#37	#38	#39	#40
	200	#41	#42	#43	#44
	300	#45	#46	#47	#48
	400	#49	#50	#51	#52

We used various techniques to observe geometrical shape of the trenches. A rough selection of the experimental results was made by means of an optical phase contrast interference microscope. The complete removal of the ITO layer, ridges formation on edges and the substrate damage were the main criteria we used for characterization. Detailed investigations of the grooves etched by laser radiation were done with the Taylor Style profiler, the scanning electron microscope (SEM) and the atomic force microscope (AFM).

Table 2 Samples of ITO on the glass substrate prepared with the PL10100 laser: laser wavelength, pulse energy and step between pulses by processing a line.

λ, nm	step, μm / energy, μJ	1	2	5	10
266	1.46	#1`	#2`	#3`	#4`
	1.08	#5`	#6`	#7`	#8`
	0.69	#9`	#10`	#11`	#12`

Surface contaminations at the bottom of trenches and of the original non-irradiated surface of ITO were controlled by the Auger spectroscopy using the surface analysis equipment LAS-3000 (Riber).

3. Results and discussion

Indium-tin oxide is transparent in the visible spectrum range. The feature is particularly important to applications of the material. When applying lasers for processing of ITO, small absorption in the VIS spectrum should be taken into account. The reflection and transmission spectra of the ITO layer on glass and the substrate without coating were measured with the spectrophotometer Lambda 950 (Perkin Elmer).

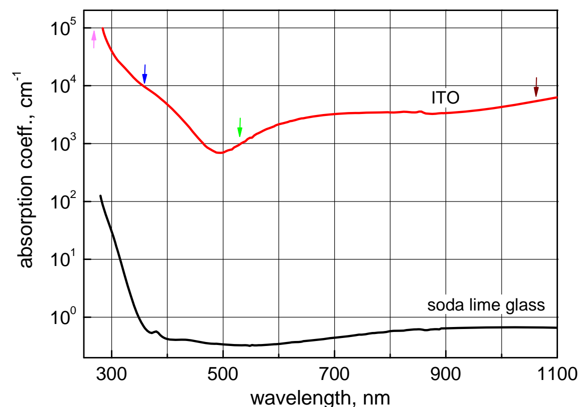

Fig. 1 Absorption spectra of the ITO and soda lime glass used in experiments evaluated from reflection and transmission spectra, measured in the ITO glass and the glass substrate without coating.

The absorption coefficient was calculated according to equation (1) and its values obtained from the spectra (Figure 1) are presented in Table 3.

$$I = I_0(1 - R_{ITO})e^{-(\alpha_{ITO}d_{ITO}+\alpha_{glass}d_{glass})} \quad (1)$$

Table 3 Absorption coefficient of ITO and the glass substrate at various laser wavelengths, evaluated from the reflectivity and optical transmission measurements.

wavelength	1064 nm	532 nm	355 nm	266 nm
α_{ITO}, cm^{-1}	5.4*10^3	1.0*10^3	1.0*10^4	>10^5
α_{glass}, cm^{-1}	0.66	0.33	0.76	1.3*10^2

Rapid increase of absorption was found in the UV range, for wavelengths shorter than 350 nm. Both the substrate of soda-lime glass (1.1 mm thick) and the ITO layer were responsible for absorption. Optical density was too high at 266 nm for measurements. The estimated value of the ITO absorption coefficient at 266 nm was higher than $1.3*10^5$ cm^{-1}. The ITO layer absorbed more than 70% of laser radiation with the thickness of 120 nm. According to [10], absorption of the ITO film with the same thickness was about 60 % at 266 nm. Similar absorption spectra of the substrate and ITO made difficulties in choosing the right processing regime. Low absorption in visible and infrared spectra required higher pulse energy to initiate ablation. The 266 nm radiation was effectively absorbed by the substrate, and therefore it could be easily damaged by radiation.

3.1 Ridges on edges of trenches

The width of trenches was measured as a function of the laser fluence. Fig. 2 shows profiles of trenches in ITO, formed by pulses of the PL2241 laser with the wavelength of 266 nm and pulse energy of 8 µJ. They were measured with the Stylus profiler. The laser fluence averaged through beam diameter is shown on the right side.

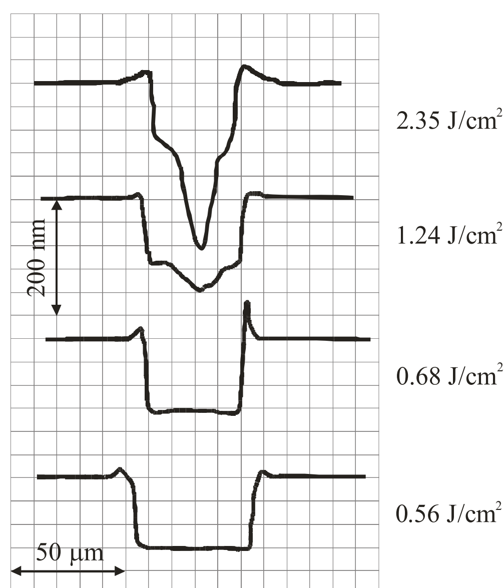

Fig. 2 Alteration in shape of the laser etched trenches in the ITO layer on the glass substrate depending on laser fluence. Sample #1 (266 nm, pulse energy 8 µJ, step 1 µm).

The ITO layer with the thickness of 120 nm was fully ablated at low energy density using the 266 nm radiation, which is well absorbed by the oxide film. The higher laser fluence intensified the material removal process. The width of trenches etched with the laser varied because of local laser fluence, the beam diameter and spot overlap that were controlled by objective movement. Even the lowest used pulse energy of the PL2241 laser at 266 nm and 355 nm (8 µJ) was high enough to cause damage of the glass substrate when it was placed near the focus. Grooves in ITO and the substrate were deep (a few µm) with high ridges around. Some part of ITO was extruded by vapor as a melt. Solidification of the melted material formed ridges on edges of the grooves.

Selected samples with trenches of the most acceptable shape and quality were tested by SEM. Typical pictures of trenches made with the 266 nm and 355 nm radiation are shown in Fig. 3. The trenches shown in the upper row of pictures were etched with 266 nm laser radiation, while the grooves in the lower one were made at 355 nm wavelength. Cases a) and c) as well as b) and d) corresponded to the same experimental conditions. It is evident that the short-wave UV radiation of 266 nm led to a better processing quality. Edges of the trenches were straight and sharp, while after the processing with 355 nm radiation a lot of debriss was observed on the ITO surface. Even at high overlap of laser pulses, the edges were rough because of spallation of the ITO layer. The quality of processing with the 532 nm radiation was even worse.

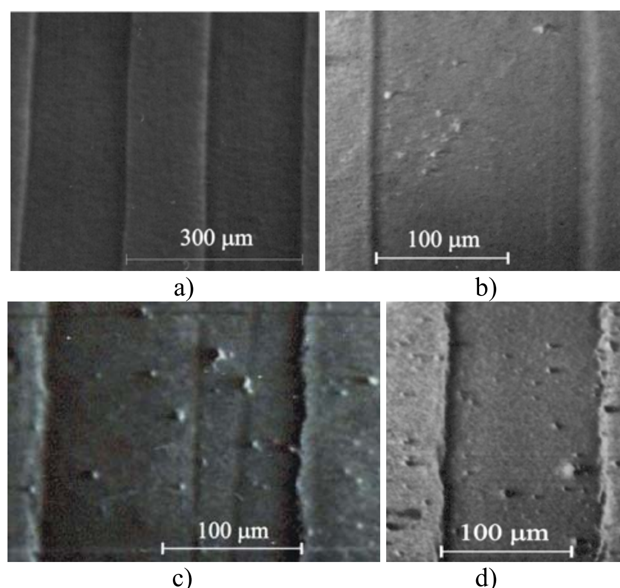

Fig. 3 SEM pictures of trenches ablated with the PL2241 laser in ITO: a) sample #6 (266 nm, 20 µJ, step between pulses 2 µm); b) sample #11 (266 nm, 40 µJ, step between pulses 5 µm); c) sample #22 (355 nm, 20 µJ, step between pulses 2 µm); d) sample #27 (355 nm, 40 µJ, step between pulses 5 µm). Z= 1.9 mm.

We used AFM for testing narrow trenches in ITO made with the high repetition rate laser PL10100 and the short focus objective. Pictures are shown in Fig. 4.

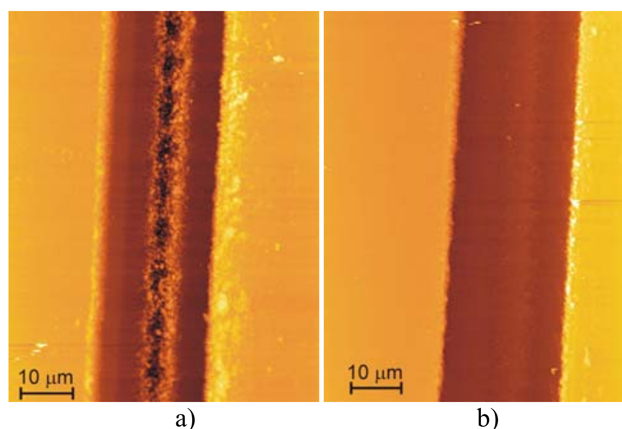

Fig. 4 AFM pictures of trenches etched with the PL10100 laser in ITO at 100 kHz. Wavelength 266 nm, laser pulse energy 0.69 µJ. a) – 0.84 J/cm²; b) – 0.58 J/cm².

Laser fluence used for etching of lines was changed by the shift of the objective. The resulting width of trenches was about 24 µm with the pulse energy of 0.69 µJ. The shift of the focus more close to the surface led to ablation of the substrate. Faster movement of the sample under the laser beam allowed us to reach the processing speed of 300 mm/s at the 130 mW average power and 100 mm/s at the 20 mW average power with the wavelength of 266 nm without damage of the glass substrate. The minimal width of separation grooves was 13 µm and 7 µm, accordingly.

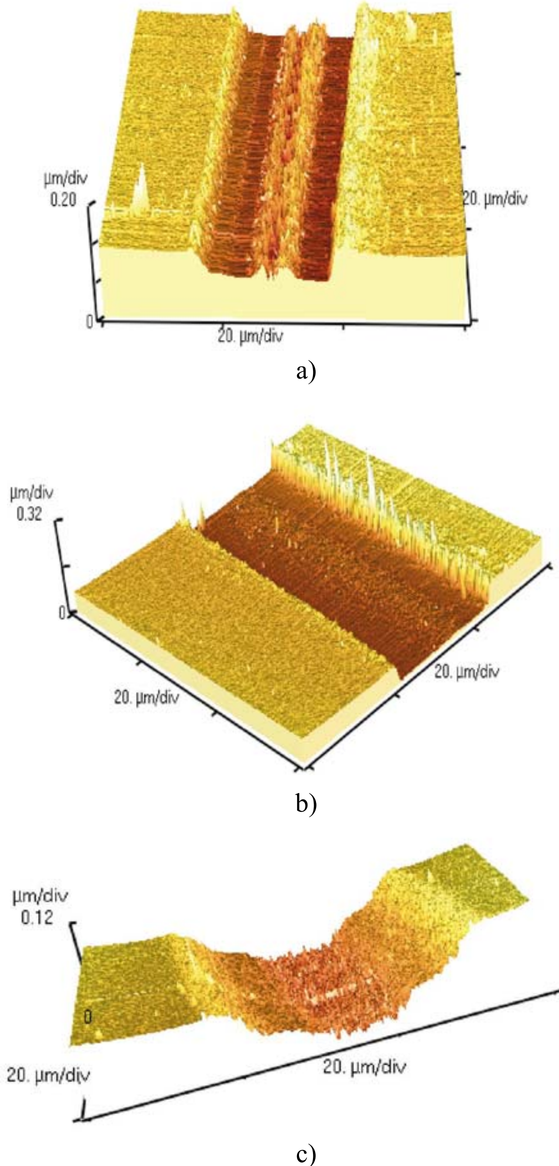

Fig. 5 AFM pictures of trenches etched with the PL10100 laser in ITO at 100 kHz. Wavelength 266 nm, laser pulse energy 0.69 µJ. a) – 0.84 J/cm^2, width 22.2 µm; b) – 0.58 J/cm^2, width 24.2 µm; c) – 0.15 J/cm^2, width 34.6 µm.

3D pictures of trenches are shown in Fig. 5. The substrate was damaged at higher laser fluence (a), while the incomplete removal of ITO was observed when the fluence was too low (c). Ridges with a height of about 50-70 nm were formed in a limited area close to the edge on one side of the trenches (b). The reason for the ridge formation on one side was slight asymmetry of the laser beam at the 266 nm wavelength. Ridges on the edges were in the range of 20-100 nm even when a femtosecond laser was used [8].

Ripples with a period of ~200 nm were found at the bottom of trenches, when the wavelength of laser radiation was 266 nm. The height of the sub-wavelength structure was up to 20 nm. The ripples were located along the trench in ITO and were formed by the incompletely removed ITO according to [5].

3.2 Ablation threshold

The width of trenches etched with laser radiation was measured and used to estimate the energy density required for the complete removal of the ITO layer. The parameter differs from the ablation threshold, the minimal laser fluence that corresponds to the beginning of material ablation. According to [8], when the ablation threshold of ITO for the 150 fs pulse duration was 0.9 J/cm^2 at 775 nm, the full removal of the 150 nm thick ITO layer was done at fluence of 2.4-4.5 J/cm^2. The threshold was estimated from the relationship between the laser fluence F and the diameter D of a crater etched by a pulse [11]:

$$D^2 = 2\omega_0^2 \ln\left(\frac{F_0}{F_{th}}\right), \quad (2)$$

where ω_0 denotes the beam waist.

We used the width of trench made by series of pulses instead of a diameter. The trenches etched at various laser pulse energies at the same height of the focus (Z) were selected. Their width was plotted versus pulse energy. The waist radius was estimated at the first step from a slope, and the pulse energy E_p was converted to the laser fluence. Linear fitting of the data was performed according to the relation $D^2 \sim ln(E_p)$. Reliability of the results was increased by repeating the procedure with various Z values (Fig. 6). The pulse overlap did not differ significantly for nearby trenches. Therefore, the lines crossed x-axis at the same point because the threshold energy was the material parameter. A large shift of the objective (Z=1 mm) decreased the pulse overlap 2.5 times and the threshold energy increased.

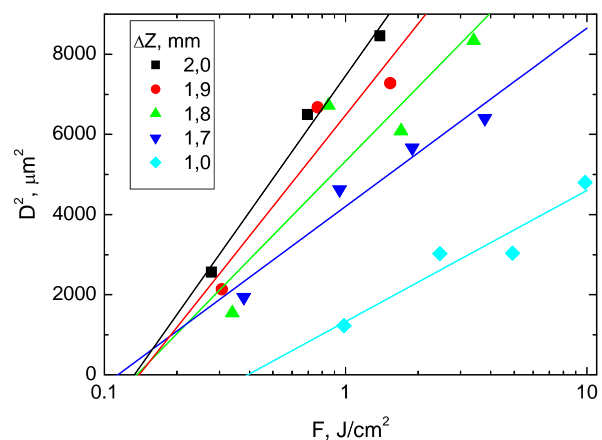

Fig. 6 Width of trenches as function of laser fluence: 266 nm, step between pulses 2 µm (samples #2, #6, #10, #14).

Such analysis was performed for all groups of samples, irradiated by different pulse energies. The ablation (removal) threshold was estimated for ITO and the damage threshold was found for the glass substrate. Data are presented in Table. 4. The values depended on the step between pulses because it had direct relation with the pulse overlap.

Table 4 The threshold fluence for removal of the indium-tin oxide layer with the thickness of 120 nm and for damage of soda-lime float glass (in J/cm^2).

	step, μm	266 nm	355 nm	532 nm
ITO	1	0,18	0,46	2,11
	2	0,13	0,34	2,57
	5	0,20	0,49	2,64
	10	0,21	0,56	3,04
glass	2	1,55	1,83	4,66
ratio glass/ITO		8,60	3,96	1,80

When the 266 nm radiation was applied, the ablation of ITO was initiated with the energy density of ~0.2 J/cm^2. For the 355 nm radiation, the threshold increased up to 0.5 J/cm^2, and for the 532 nm radiation, it was even 2-3 J/cm^2. The ablation threshold of the glass substrate also increased with the wavelength of laser radiation. However, the ratio of the ablation thresholds of glass and ITO fell down with the increase in the wavelength. In this aspect, the 266 nm radiation was more attractive for patterning of ITO on glass because the working window was larger. The ablation threshold here corresponds to the energy density required for the complete removal of the 120 nm thick layer of ITO.

The change in the trench width by shifting the objective (Z) reflected variation in laser fluence with a beam diameter. The behaviour was modeled for the Gaussian beam near its waist. Radial distribution *F(r)* of the Gaussian beam could be described as:

$$F(r) = F_0 e^{-\frac{2r^2}{\omega_0^2}}, \tag{3}$$

where r is the radius, ω_0 is the beam waist (at $1/e^2$ level) and, F_0 is the energy density (fluence) at the beam center. Laser fluence is related to the pulse energy:

$$F_0 = \frac{2E_p}{\pi\omega_0^2}. \tag{4}$$

Behaviour of the Gaussian beam near its waist can be described only by the waist radius. The highest laser fluence is at the beam waist in the beam center. By focusing with a lens, the beam converges before the waist and diverges after passing it. Variation in the beam radius could be expressed by relation:

$$\omega(z) = \omega_0\sqrt{1+\left(\frac{\lambda z}{\pi\omega_0^2}\right)^2}, \tag{5}$$

where z is the distance from the waist. The ablation takes place in areas where the local laser fluence exceeds the ablation threshold F_{th}. The radius of the area could be found according to the equation:

$$r_A(z) = \frac{\omega(z)}{\sqrt{2}}\sqrt{\ln\left(\frac{2E_p}{F_{th}\pi\omega^2(z)}\right)}. \tag{6}$$

We used equation (6) to calculate the predictive width of trenches depending on the ablation threshold. Some results compared with experimental values for 266 nm wavelength are presented in Fig. 7.

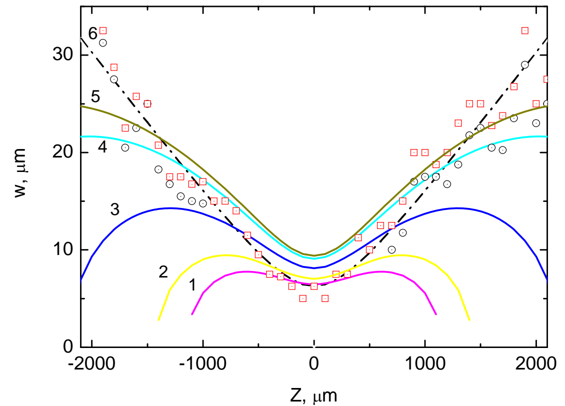

Fig. 7 Isoenergetic lines of the Gaussian beam near its waist and the width of trenches (dots) etched with a focused beam in various focal positions relative to the surface. Sample #1, 266 nm, 8 μJ, step 1 μm. Laser fluence: 1 – 1.55 J/cm^2; 2 – 1.05 J/cm^2; 3 – 0.45 J/cm^2; 4 – 0.20 J/cm^2; 5 – 0.15 J/cm^2; 6 – Gaussian beam with the waist of 6 μm.

The real width of the trenches was in agreement with predictions of the ablation threshold of 0.15-0.2 J/cm^2, when the energy density was not too high to initiate ablation of the substrate at the beam center (Z=1-2 mm). Residue of glass at high laser fluence covered the real trench in ITO, and the observed and measured width of trenches was the width of the groove in the substrate with the threshold fluence of 1.55 J/cm^2. A better agreement with theoretical predictions was found when the multiple pulse overlap was taken into account.

The 532 nm radiation was badly absorbed by ITO. Therefore, high pulse energies (more than 40 μJ) were required to initiate the ablation under the same focusing conditions.

3.3 Surface contamination

Special experiments were performed in order to estimate the quality of the laser processing. Change in composition of the compound oxide during the laser ablation was investigated by the Auger electron spectroscopy (AES). The spectra were measured on the bottom of the trench and compared with AES spectra of non-processed ITO near the edges. The spectra are presented in Figs.8 and 9.

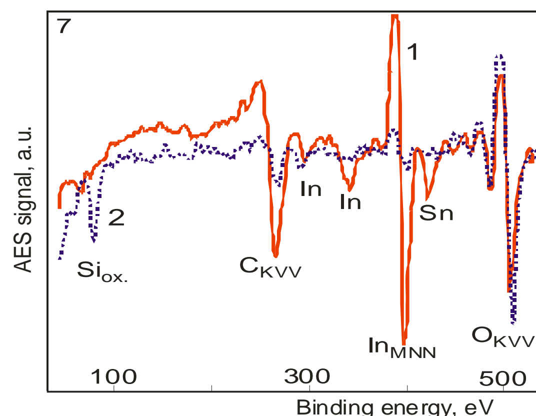

Fig. 8 AES spectra measured on the ITO surface (1) and at the bottom of trenches etched with the laser (2). Sample #7, 266 nm, laser pulse energy 20 μJ, step 5 μm.

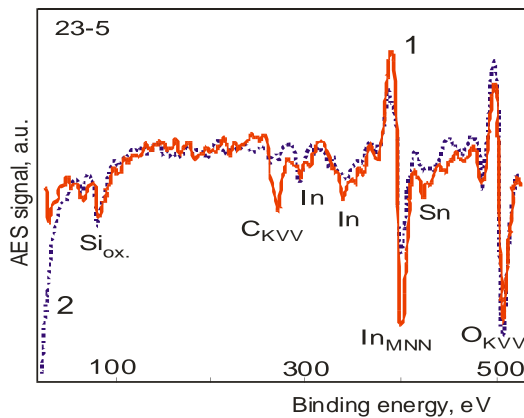

Fig. 9 AES spectra measured on the ITO surface (1) and at the bottom of trenches etched with the laser (2). Sample #23, 355 nm, laser pulse energy 20 µJ, step 5 µm.

Lines corresponding to the emission of Auger electrons by indium and tin atoms were found in AES spectra. They were observed both in the ITO layer and at the bottom of trenches as residue of the ablation process. The origin of the Si line was silicon oxide, the main material of glass. Its evidence in AES spectra is an indicator of the complete removal of the ITO layer. Oxygen is incorporated into both ITO and glass, but the carbon line is caused by the surface contamination with organic materials.

By comparing AES spectra measured in samples prepared with 266 nm and 355 nm laser radiation, maintaining all other experimental conditions identical (Fig.8 and Fig.9), indium-tin oxide was removed more efficiently and clean with the 266 nm UV light. In fact, no In or Sn were observed at the bottom of the trench. The 335 nm radiation under the same conditions was not able remove completely the ITO layer due to the lower absorption and higher ablation threshold. The quality of removal became even much worse when laser fluence was increased by decreasing the distance Z to the focal plane of the objective. As the energy density exceeded significantly the ablation threshold, the bad quality was related to splattering of the material. Residues of ITO and glass were spread all over the surface. An indicator of the spreading was Si-oxide line on the ITO surface. This means that even close to the ablation threshold the substrate was ablated using the 355 nm radiation, while for 266 nm radiation far away from the threshold, the patterning was only in the ITO layer.

4. Conclusions

Picosecond lasers were used for patterning of ITO on the glass substrate. Depending on the local laser fluence and wavelength, the quality of processing was different. Clean removal of the ITO layer at the 266 nm radiation was observed above the threshold of 0.20 J/cm^2. The processing speed was up to 0.5 m/s when the average power of the laser was 150 mW at the 100 kHz pulse repetition rate. The minimal width of the trench was 7 µm.

The ablation threshold for the 355 nm radiation was higher, above 0.46 J/cm^2. Spallation of the ITO layer led to rough edges of trenches. Edges of trenches were found to be thermally affected by the use of 532 nm radiation.

The glass substrate was damaged in places where the fluence was higher than 1.55 J/cm^2. The processing parameters should be carefully selected because the substrate can be damaged when the laser fluence is too high. The 266 nm radiation provided a wider processing window.

The use of fluences close to the ablation threshold made it possible to minimize the recast ridge formation and surface contamination during the process. The latter was confirmed by the scanning Auger spectroscopy.

UV picosecond lasers with the high repetition rate were found to be a good alternative to conventional photolithography for flexible patterning of ITO.

Acknowledgment

The work was supported by the Lithuanian State Science and Studies Foundation under project No B21/2006.

References

[1] T.L. Breen, P.M. Fryer, R.W. Nunes, M.E. Rothwell, Langmur, **18**, (2002) p. 194-197.

[2] J.N. Bardsley, IEEE Selected Topics in Quantum Electronics, **10**, (2004) p. 3-9.

[3] C. Molpeceres, S. Lauzurica , J.L. Ocana, J.J. Gandia, L. Urbina, J. Carabe, J. Micromech. Microeng. **15**, (2005) p.1271-1278.

[4] M. Henry, P. M. Harrison, J. Wendland, LAMP 2006, May 16-19, Kyoto, Japan. (2006).

[5] O. Yavas, M. Takai, J.Appl.Phys., **85**, (1999) p.4207-4212.

[6] O.A. Ghandour, D. Constantinide, R. Sheets, Proc SPIE, **4637,** (2002) p.90-101.

[7] M.Y. Xu, J. Li, L.D. Linge, P.R. Herman, Appl. Phys.A, **85** (2006) 7.

[8] H.W. Choi, D. Farson, K.R. Kim, Proc. of 6th Int. Symp. on Laser Precision Microfabrication LPM 2005, Williamsburg, USA, (2005) p.58-63.

[9] R. Tanaka, T. Takaoka, H. Mizukami, T. Arai, Y. Iwai, Proc. of SPIE **5063**, (2003) p.370-373.

[10] D. Ashkenasi, A. Rosenfeld, Proc. SPIE **4637**, (2002) p.169-179.

[11] P.T. Mannion, S. Favre, D.S. Ivanov, G.M. O'Connor, T.J. Glynn, Proc. of 3-rd Int. WLT-Conference on Lasers in Manufacturing 2005, Munich, June 2005.

(Received: May 16, 2006, Accepted: December 20, 2006)